Comparative Study of Carbon Dioxide and Methane Adsorption by Synthesized Fine Particles of SAPO-34 Molecular Sieve

Ashraf Talesh, Sayed Siamak; Fatemi, Shohreh*+; Hashemi, Sayed Jalal;
Emrani, Peyman

Oil and Gas Excellence Department, Faculty of Chemical Engineering, University of Tehran,
P.O. Box 11155-4563 Tehran, I.R. IRAN

ABSTRACT: *Fine particles Silicoaluminophosphate-34 were synthesized by hydrothermal sol-gel method. The effect of crystallization time, as one of the important synthesis factors on particle size and crystallinity, kinetic and equilibrium adsorption, and selectivity of CO_2 / CH_4 has been studied in this work. The adsorption isotherms are obtained at moderate gauge pressures (100-3000 kPa) and temperatures (278, 288 and 298 K), and the equilibrium adsorption parameters as well as heat of adsorption are determined for the synthesized SAPO-34. The observed adsorption selectivity of CO_2 to CH_4 was determined to be around eight for that sample with higher degree of crystallinity. The crystallinity, isotherm parameters, adsorption selectivity and heat of adsorption confirm that the synthesized fine particle of SAPO-34 could be a good candidate for separation of CO_2 from CH_4.*

KEY WORDS: *SAPO-34, Adsorption, Crystallization, Carbon dioxide, Methane, Fine particles.*

INTRODUCTION

Because of the undesirable effects of CO_2 in gaseous mixtures, separation of carbon dioxide from methane is an important technical challenge in economical and environmental affairs. CO_2 is present in atmosphere, natural gas and by-products of industrial processes. CO_2 decreases the energy content of natural gas and because of its acidic property, causes corrosion in storage and transportation systems. Therefore, according to the increasing trend in consumption of natural gas, containing CH_4 as the major component, removal of CO_2 has a vital role in the industries dealing with natural gas processing. The process of amine washing is a traditional method of removing CO_2 whereas this process is a hazardous and environmental unfriendly technique [1]. Adsorption process is an economic and effective method with wide usage in separation of gaseous mixtures. Appropriate adsorbent selection is one of the main and important steps in effective adsorption processes. Nowadays, microporous materials are being studied as good alternatives in separation processes [2].
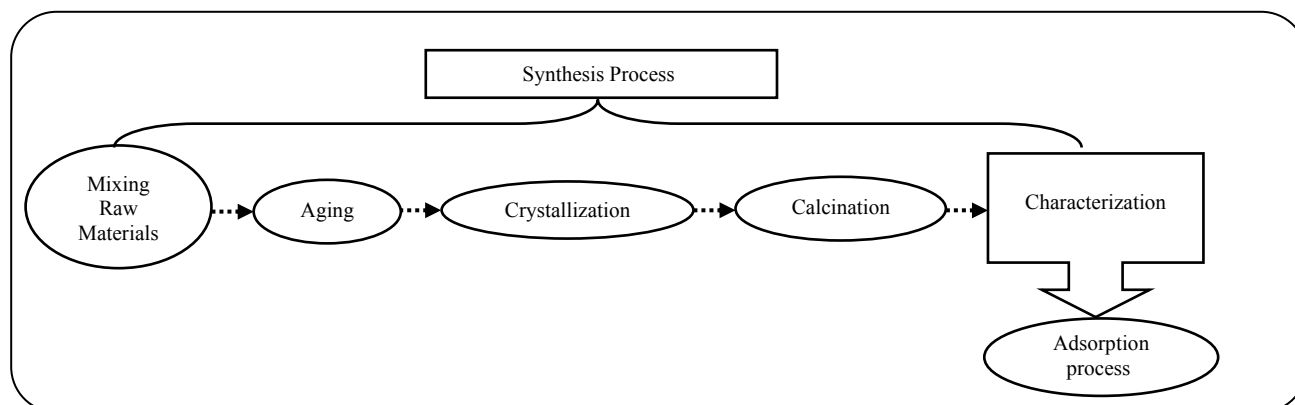
Fig. 1: Scheme of experimental procedure.

Molecular sieves such as zeolites and zeo-types (silicoaluminophosphate) nonporous materials apart from their high thermal, mechanical and chemical stability, have the unique property that only molecules with a smaller kinetic diameter than the pores' diameter can diffuse into the channels of the adsorbents, therefore they can act as sieving to the gaseous mixtures. Zeolites have an inorganic crystalline structure with uniform pore size distribution [3].

Silicoaluminophosphates (SAPOs) are from ALPOs categories and have similar structure to zeolites except for substitution of Si with Al in their cages. SAPO molecular sieves have excellent efficiency in catalytic and separation processes such as adsorption and membrane processes [4,5]. The kinetic diameter of the gas component is the key parameter in its ability to diffusion into the pores of the adsorbents. Within many types of SAPOs, SAPO-34 with a three-dimensional structure and pore diameter of 0.38 nm is selected, in this research, as the best candidate for selective adsorption of CO_2, with 0.33 nm kinetic diameter, from CH_4, with 0.38 nm diameter. It should be noted that SAPO-5, SAPO-41, SAPO-11, etc. are one-dimensional and have a pore size larger than 0.38 nm and would let both CO_2 and CH_4 move through the pores, without any separation [6]. Although there have been found some remarkable studies on SAPO-34 in recent years, they are usually limited to membrane studies [7-13].

The scope of this research is to prepare fine particles of SAPO-34, in order to be used as an efficient adsorbent in the adsorption separation process for separation of CO_2 and CH_4.

In this work the effect of crystal size reduction to submicron on the kinetic adsorption, equilibrium and selectivity of CO_2 over CH_4 has been studied. At First fine particles of SAPO-34 are synthesized by hydrothermal procedure at two different crystallization times to figure out the effect of crystallization time on particle size and crystallinity. Thereafter, kinetics and equilibrium adsorption of CO_2 and CH_4 are examined by the volumetric method in an adsorption set up and batch adsorption properties are determined in various pressures and temperatures.

EXPERIMENTAL SECTION

The schematic of synthesis procedure is shown in Fig. 1. At first the fine particles of SAPO-34 are synthesized and then tested in the adsorption process to find out their efficiency.
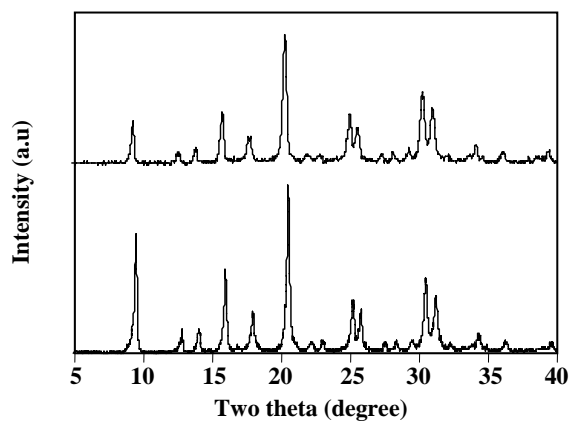
Synthesis

SAPO-34 samples were synthesized by the hydrothermal transformation from a gel with molar composition of $1Al_2O_3$; $0.4SiO_2$; $1P_2O_5$; $2TEAOH$; $50H_2O$, corresponding to a Si/Al ratio of 0.2. The sources for the preparation of the initial precursors were phosphoric acid (85 wt% aqueous solution, Merck), aluminium isopropoxide (Merck), silica gel 60 (Merck) and Tetra-Ethyl Ammonium hydroxide (TEAOH, 35% wt aqueous solution, Aldrich) as template agent.

The gel was prepared by mixing deionized water, phosphoric acid and slowly adding aluminium isopropoxide under high stirring in order to dissolving aluminium, then silica gel and TEAOH were added, respectively. Afterwards, the mixture was aged for 24 h under agitation at room temperature. After aging, the gel was placed in a Teflon lined autoclave and the crystallization process was carried out at 463K with different crystallization

Table 1: Synthesis conditions of the two samples.

Samples	Crystallization Time(h)	Crystallization Temperature(K)	Calcination Temperature(K)	Calcination Time(h)
A₁	24	463	823	7
A₂	48	463	823	7

Fig. 2: XRD pattern of samples, (a) A₁; (b) A₂.

times (24, 48 h). The synthesized samples were washed with deionized water and centrifuged many times until the pH of the solution approached to around seven, after which the calcinations were carried out in a static air furnace at 823 K for 7 h as shown in Table 1.

Characterization

Calcined powder of SAPO-34 was characterized by the XRD and SEM. The XRD pattern was recorded on a Philips analytical X-ray diffractometer with Cu Kα radiation (λ=1.54 °A) and the crystal morphology was analyzed by Scanning Electron Microscopy (SEM, S-4700) as shown in Figs. 2 and 3, respectively.

Adsorption experiment

A schematic diagram of the hand made adsorption set-up is shown in Fig. 4, by which the kinetic and equilibrium adsorption experiments were carried out by volumetric method. The pipe line and the cells are stainless steel and the system can operate at different temperatures and pressures up to 7000 kPa. The Volume of reference gas vessel and adsorption cell are 230 and 85 cm³, respectively. In order to determine the adsorption capacity and isotherms, the samples were placed in the adsorption cell. Pressures were measured using pressure transducer with precision of 10 kPa. Temperatures in respective cells were controlled to within 1K.

Adsorption

After loading the adsorbents (A₁ or A₂) into the adsorption cell and pretreatment at 423 K under vacuum condition for five hours, the adsorption tests were carried out, at three various temperatures (278, 288, 298 K) and gage pressures (100, 500, 1000, 1500, 2000, 2500, 3000 kPa) for carbon dioxide and methane. The amount of gas adsorption was measured by recording the system pressure, using the high precise pressure sensor, before and after equilibrium. Experiments were conducted with kinetic adsorption followed by the equilibrium condition. Setting the temperature of the adsorption cell at a desired level, the batch experiment was started with a known amount of inlet gas into the adsorption cell and the pressure sensor recorded the variation of the pressure against time until it achieved a constant level. Difference between the initial pressure and recorded pressure at any time was used for calculation of the adsorbed amount using the real gas calculation. The ultimate pressure without any change was reported as the equilibrium condition. The detailed procedure has been mentioned elsewhere [14].

MODEL DESCRIPTION

For light gases on molecular sieves, Langmuir single-site adsorption can be used as an equilibrium model [2]:

$$\theta = \frac{q_i}{q^{sat}} = \frac{bp}{1+bp} \tag{1}$$

Pure component parameters of Langmuir isotherm according to the experimental data in any temperature and full range of equilibrium pressures were derived and presented in Table 2. Comparison between experimental and model values is based on the absolute average relative deviation (% AARD).

$$AARD\% = \frac{1}{N_d} \sum_1^N \left| \frac{q_{i,exp} - q_{i.model}}{q_{i,exp}} \right| \times 100 \tag{2}$$

RESULTS AND DISCUSSION

Synthesis Results

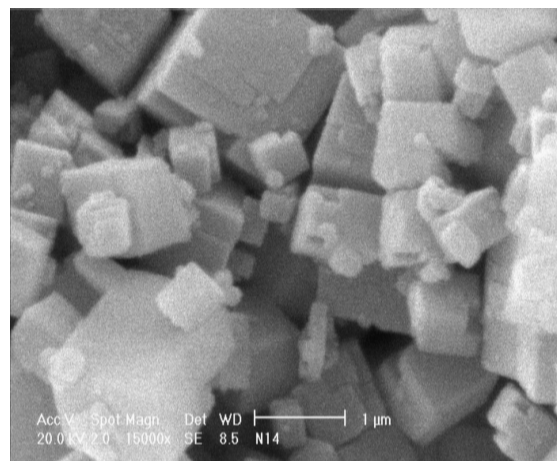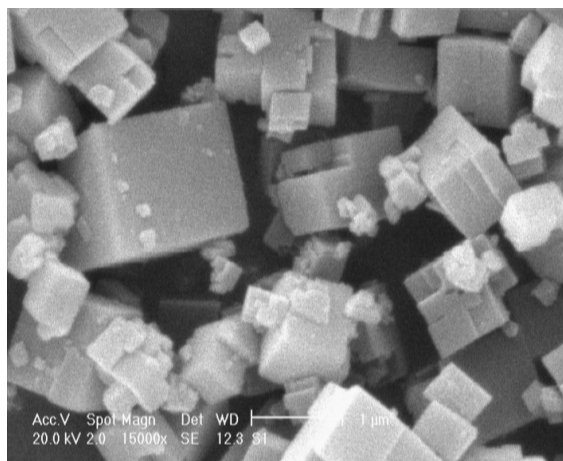XRD patterns and SEM graphs are presented in Figs. 2 and 3, respectively. The XRD patterns with well

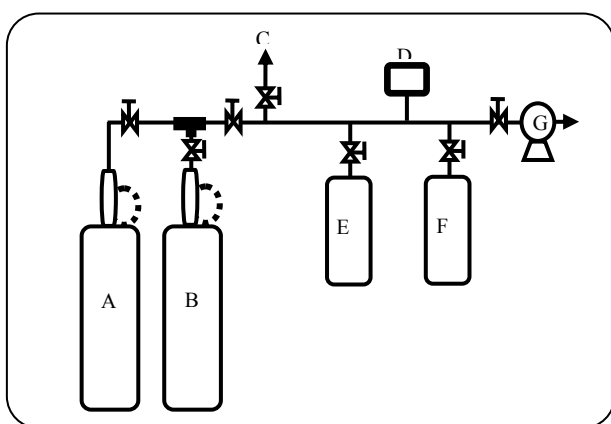*Fig. 3: SEM photographs of the samples surfaces; (a) A_1 , (b) A_2 .*

Fig. 4: Schematic diagram of experimental apparatus: A: (CO_2 or CH_4) Cylinder; B: Helium Cylinder; C: vent; D: Pressure transducer(0-3000 kPa); E: Reference gas vessel; F: Adsorption cell; G: Vacuum pump.

known AAPO-34 Peaks and SEM graphs with cubic shapes of crystals in the range of 300 nm to 1μm, confirm the formation of submicron crystals of SAPO-34. Comparison between the SEM graphs reveals nonsignificant difference in the size of the samples. The height of the peaks in XRD patterns for sample A_2 is observed sharper than sample A_1. This fact reveals more crystallinity of the sample A_2 that can be explained because of 48 h crystallization time for A_2 compared to the lower time of crystallization for sample A_1. It is concluded that crystallization time in hydrothermal method could be an effective parameter to approach to the higher crystal intensity [15]. The effect of improvement in crystallinity can be observed in the adsorption process because higher crystallinity means good adsorption efficiency. Although both adsorbents have shown good

efficiency of adsorbing CO_2 compared to CH_4, sample A_2 is more selective for CO_2 than A_1.
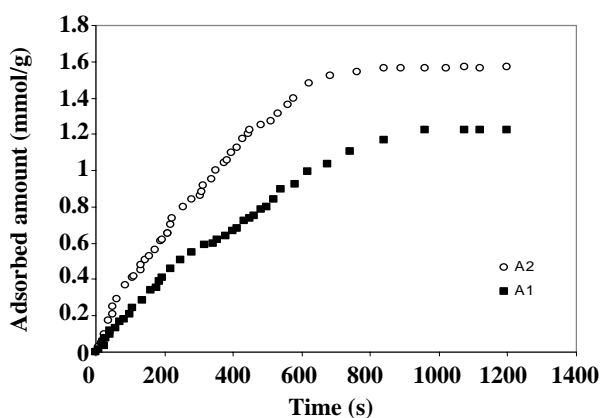
Adsorption Results

The isotherm curves at various pressures and temperatures show that the adsorption capacity of CO_2 is greater than that of CH_4, presented by Figs. 6 to 9. This result is reasonable because of the kinetic diameter of CO_2 (0.33 nm) compared to CH_4 (0.38 nm), therefore CO_2 can enter through the pore mouth of SAPO-34 crystals with diameter of 0.38 nm. Another reason of CO_2 good adsorption on SAPO-34 is its surface properties and especial characteristics of CO_2 and CH_4. Methane is a non-quadrupole molecule, whereas CO_2 has a strong quadrupole moment and because of the shape and electrostatic interactions, higher adsorption capacity can be observed [8]. On the other hand, it can be said that the more positive charges in the crystal structure of SAPO-34 and the more heterogeneity of the surface could be a dominant factor in attractive forces with CO_2.

Adsorption Isotherms

Before the equilibrium condition, there is diffusion resistance inside the pores which causes the kinetic adsorption through the adsorbent. Fig. 5 exhibits variation of adsorbed amount of CO_2 on the A_1 and A_2 at 298 K and first point of operating pressure. It is obvious that the rate of CO_2 adsorption in A_2 is faster than that in A_1. The time of approaching to the equilibrium condition is determind around 60 min for sample A2, whereas it takes about 80 min for sample A1, it means the material with higher crystallinity can adsorb CO_2 more rapidly with higher kinetic rate.

Table 2: Langmuir model parameters of the samples.

	T=298 K	T=288 K	T=278 K
Sample A_1			
CH_4			
q^{sat} (mmol/g)	4.52	5.31	5.13
$b*100$ $(kPa)^{-1}$	0.047	0.041	0.056
%AARD	2.62	3.43	2.51
CO_2			
q^{sat} (mmol/g)	9.70	11.06	12.30
$b*100$ $(kPa)^{-1}$	0.141	0.140	0.173
%AARD	5.22	6.20	6.09
Sample A_2			
CH_4			
q^{sat} (mmol/g)	5.67	6.84	7.70
$b*100$ $(kPa)^{-1}$	0.042	0.038	0.039
%AARD	2.57	3.64	4.01
CO_2			
q^{sat} (mmol/g)	13.78	15.76	18.18
$b*100$ $(kPa)^{-1}$	0.117	0.124	0.123
%AARD	4.29	5.22	3.18

Fig. 5: Kinetic adsorption of CO_2 on the A_1 and A_2 at atmospheric pressure.

Isotherm data of methane and carbon dioxide are presented respectively in Figs. 6 to 9 for adsorbents A_1 and A_2. As shown in these figures the isotherm data of both adsorbates are well described by the Langmuir models. The b values for carbon dioxide were higher than that of methane which implies the higher equilibrium adsorption constant at the same temperature and more adsorption-desorption interaction for carbon dioxide in

comparison with methane. According to the results of Table 2, the order of magnitude of q^{sat}, the maximum capacity, for carbon dioxide is higher than that of calculated for methane. This fact also confirms the higher interaction and more strong attractive forces of carbon dioxide molecules with surface.

As the isotherm curve Figs. 6 to 9 show, increasing the adsorption temperature causes a decrease in the adsorption capacity, which is a reasonable result since adsorption is an exothermic process.

Adsorption selectivity was calculated from the ratio of equilibrium adsorption capacity of gases [16-18]:

$$\text{Adsorption selectivity} = \qquad\qquad (3)$$
$$\{[\text{mmol}\,CO_2\,/\,\text{g Adsorbent}]\,/\,[\text{mmol}\,CH_4\,/\,\text{g Adsorbent}]\}_{T,P}$$

As shown in these figures the adsorption selectivity increased with decreasing temperature for both adsorbents (A_1 and A_2), whereas pressure increasing affects the adsorption selectivity with a reverse manner. Figs. 10 and 11 obviously present ability of adsorption selectivity in normal pressures rather than high pressures for this kind of adsorbent in which the dynamic adsorption process might become an economic process.

According to adsorption isotherms in the studied temperature range, CH_4 and CO_2 adsorption capacity increased with increasing pressure and decreasing temperature, whereas this elevation is more in CH_4 adsorption , therefore at higher pressures selectivity of CO2/CH4 is decreased. On the other hand, due to the adsorption selectivity figures it can be seen that the adsorption selectivity is not very sensitive to the pressures of more than 1000 kPa. As a result, in the studied temperature range, adsorption selectivity is not affected by the pressure and temperature variations, mean while increasing pressure and decreasing temperature enhances adsorption capacity of each component.

Selectivity charts show a higher selectivity for A_2 compared to that of A_1, which is reasonable for better crystal intensity of A_2. For the apparent difference between performance of the two absorbent; adsorption capacity and selectivity were plotted at 298 K in Figs. 12 and 13, respectively. Fig 13 reveals that the highest selectivity of CO_2 versus CH_4 has appeared at atmospheric pressure, the lowest studied pressure. Generally the trend of adsorption results is in conformity with previous works [5, 11].
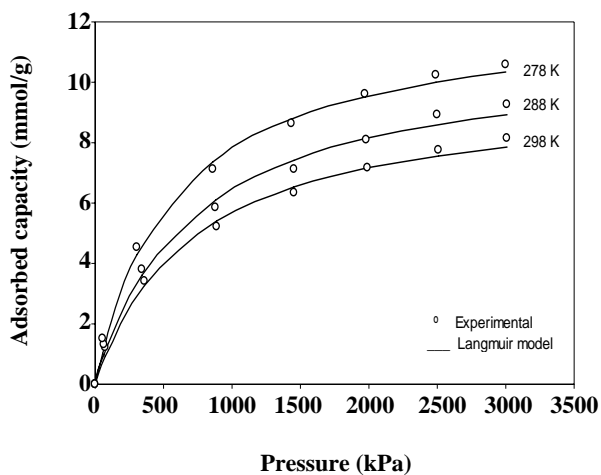
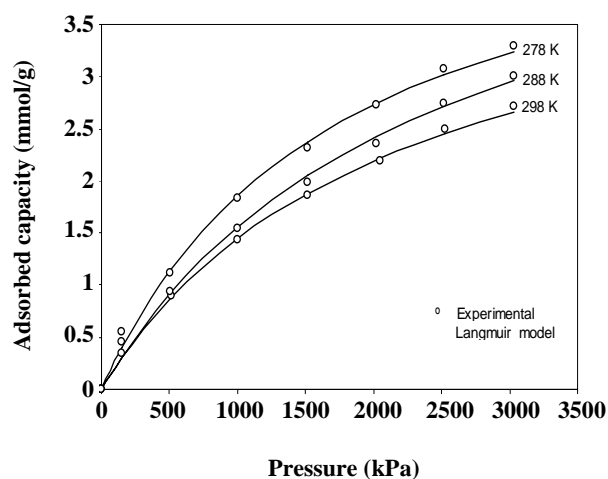*Fig. 6: Adsorption isotherm for CO_2 on A_1 adsorbent.*
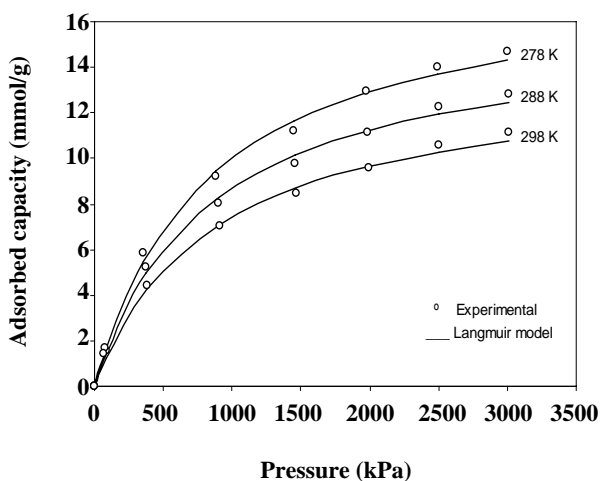

Fig. 7: Adsorption isotherm for CH_4 on A_1 adsorbent.

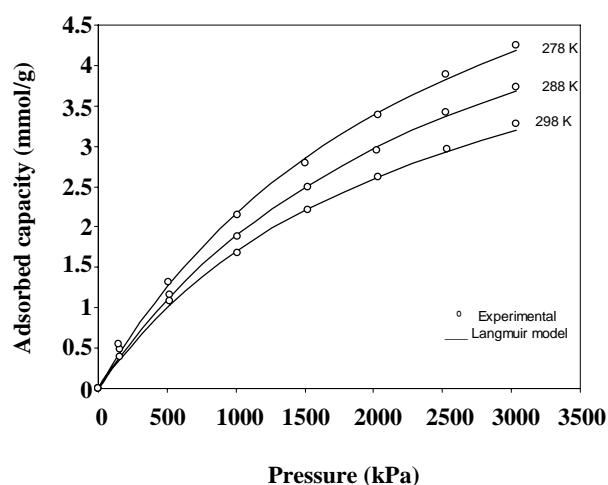*Fig. 8: Adsorption isotherm for CO_2 on A_2 adsorbent.*

Fig. 9: Adsorption isotherm for CH_4 on A_2 adsorbent.
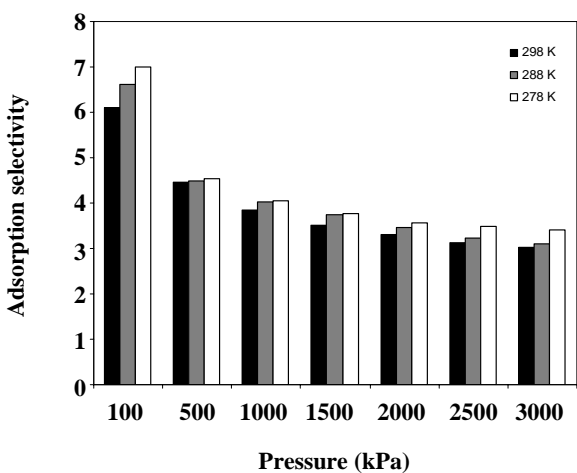

Fig. 10: Adsorption selectivity chart for A_1 adsorbent.
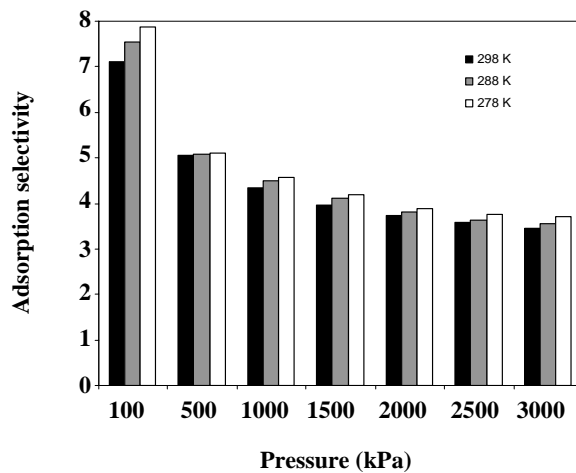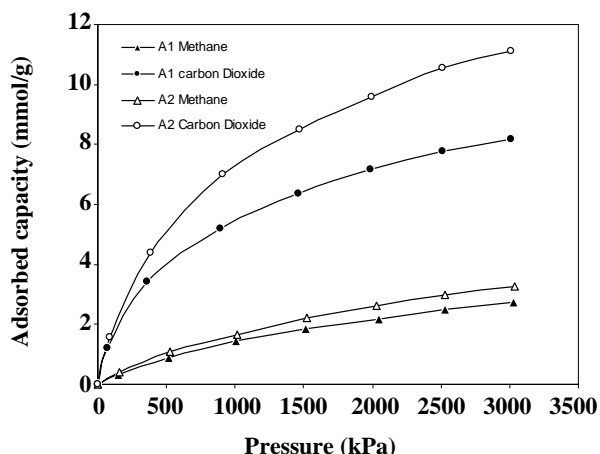

Fig. 11: Adsorption selectivity chart for A_2 adsorbent.

Fig. 12: Adsorption isotherm for CH_4 and CO_2 on A_1 and A_2 adsorbents at 298 K.

Fig. 13: Adsorption selectivity chart for A_1 and A_2 adsorbents at 298 K.

Heat of adsorption

Information related to the heat of adsorption and its variation with coverage can provide useful information about surface characteristics and the adsorbed phase. The heat of adsorption, ΔH_{ads}, was calculated from Vant Hoff equation using the experimental data:

$$\left(-\Delta H_{ads}\right)_i = RT^2 \left(\frac{\partial \ln P}{\partial T}\right)_{q_i} \tag{4}$$

In Figs. 14 and 15, the heats of adsorption for the two samples are shown as a function of adsorption capacity. Based on these figures, CO_2 heat of adsorption shows more variation in comparison with CH_4. The range of these variations is a criterion for the surface adsorbents homogeneity. Since CO_2 has more quadrupole moment in comparison to CH_4 as a non polar molecule, it has more tendencies of adsorption on heterogeneous surfaces. Due to this fact, the CO_2 / CH_4 adsorption selectivity is higher for both adsorbents.

Furthermore, these figures depict that increasing the adsorption capacity causes a reduction of the heat of adsorption. This reduction implies that the strong adsorption sites in comparison to weaker ones are occupied first.

The average heat of adsorption in the range of adsorption capacity is calculated as follows:

$$\left(-\Delta H_{ads}\right)_{av} = \frac{\sum q_i \cdot \left(-\Delta H_{ads}\right)_i}{\sum q_i} \tag{5}$$

The amount of $(\Delta H_{ads})_{av}$ is reported in Table 3.

According to the results obtained in Table 3, the heat of adsorption for the two gases is similar for both

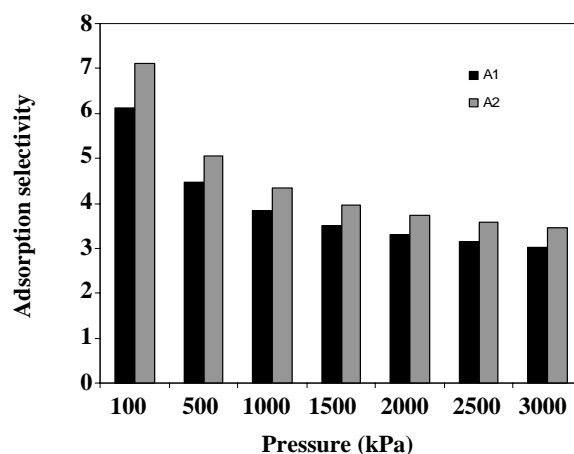samples, and there is no significant difference between the molar adsorption enthalpy of the produced samples.

CONCLUSIONS

According to the results, the degree of crystallinity of SAPO-34 are important factors in the adsorption and separation of molecules. The more crystallinity of the material, the more adsorption capacity, and it is concluded that increasing the crystallization time can improve the crystallinity of the formed phase.
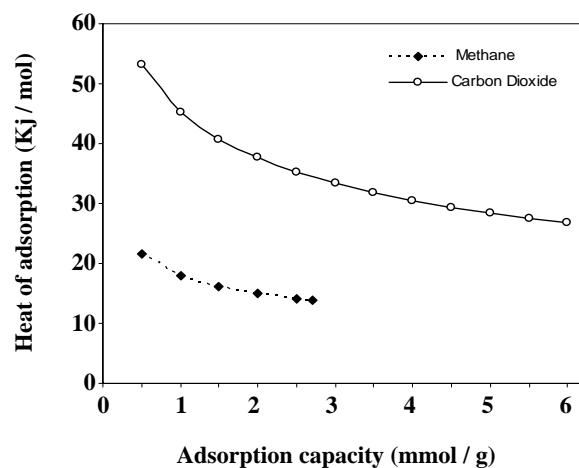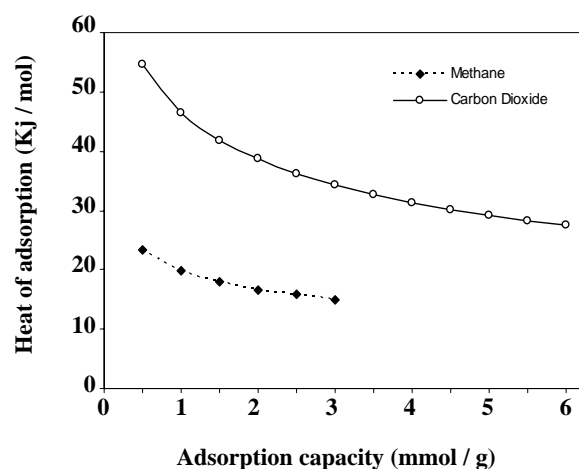
Based on the results of adsorption isotherms and adsorption selectivity, both A_1 and A_2 represent good performance in adsorption process, and this is noteworthy that adsorption selectivity of prepared samples is higher than the prior works. However the SAPO-34 product with high crystallinity and lower particle size showed the more selectivity and the more adsorption rate of CO_2 versus CH_4. In conclusion, fine particles of synthesized SAPO-34, sample A_2 in this study, can be regarded as a good adsorbent, with lower mass transfer resistance and higher CO_2/CH_4 adsorption selectivity, for enrichment of natural gas and purification of CH_4 from CO_2. To capture the efficiencies of prepared adsorbent more precisely, applying dynamic method in separation of CO_2 from CH_4 is advised in the next works.

Nomenclature

B	Gas solid interaction parameter, kPa^{-1}
I	Index of components (i= CO_2, CH_4) [-]
N_d	Number of data points [-]

Table 3: Average heat of adsorption (-ΔH_ads) av (kJ /mol).

Adsorbent		
Adsorbate	A$_1$	A$_2$
CH$_4$	16.15	16.95
CO$_2$	28.66	29.84

Fig. 14: Heat of adsorption versus adsorption capacity for A$_1$.

Fig. 15: Heat of adsorption versus adsorption capacity for A$_2$.

P	Pressure, kPa
q$_i$	Adsorption capacity of components, mmol/g
q^{sat}	Saturation adsorption capacity, mmol/g
q$_{i,exp}$	Experimental adsorption capacity, mmol/g
q$_{i,model}$	Model adsorption capacity, mmol/g
T	Temperature, K
Θ	Fractional adsorption capacity [-]

(-ΔH$_{ads}$)$_i$	Heat of adsorption of component, kJ /mol
(-ΔH$_{ads}$)$_{av}$	Average heat of adsorption, kJ /mol

REFERENCES

[1] Baker R.W., Future in Directions of Membrane Gas Separation Technology, *Ind. Eng. Chem. Res.*, **41**, 1393 (2002).

[2] Yang R.T., "Gas Separation by Adsorption Processes, Butterworth", Stoneham, p. 10 (1997)**.**

[3] Vansant E.F., **"**Pore Size Engineering in Zeolites", John Wiley & Sons, p. 145**,** (1990).

[4] Martens J.A., Grobet P.J., Jacobs P.A., Catalytic Activity and Si, Al, P Ordering in Microporous Silicoaluminophosphates of the SAPO-5, SAPO-11, and SAPO-37, *J. of Catal.*, **126**, p. 299 (1990).

[5] Li S., Falconer J.L., Noble R.D., Improved SAPO-34 Membranes for CO2/CH4 Separations, *Adv. Mater.*, **18**, p. 2601 (2006).

[6] Bennet J.M., Cohen J.P., Flanigen E.M., Pluth J.J., Smith J.V., Theoretical Studies on Aluminophosphate-5 (AlP04-5), *Am. Chem. Soc. Symp*. (1983).

[7] Walton K.S., Abney M.B., LeVan M.D., CO$_2$ Adsorption in Y and X Zeolites Modified by Alkali Metal Cation Exchange, *Micro. and Meso. Mat.*, **91**, p. 78 (2006).

[8] Himeno S., Tomita T., Suzuki K., Yoshida S., Characterization and Selectivity for Methane and Carbon Dioxide Adsorption on the all-silica DD3R Zeolite, *Micro. and Meso. Mat.*, **98**, p. 62 (2007).

[9] Li P., Tezel F.H., Adsorption Separation of N$_2$, O$_2$, CO$_2$ and CH$_4$ Gases by β-Zeolite, *Micro. and Meso. Mat.*, **98**, p. 94 (2007).

[10] Harlick P.J.E., Tezel F.H., Adsorption of Carbon Dioxide, Methane and Nitrogen: Pure and Binary Mixture Adsorption for ZSM-5 with SiO$_2$/Al$_2$O$_3$ Ratio of 280, *Sep. and Puri. Tech.*, **33**, p. 199 (2003).

[11] Hong M., Li S., Funke H.F., Falconer J.L., Noble, R.D. Ion-Exchanged SAPO-34 Membranes for Light Gas Separations, *Micro. and Meso. Mat.*, **107**, p. 140 (2007).

[12] Mertens M., Strohmaier K.G., Nurray P., Process for Manufacture of Molecular Sieves, *US. Pat. No. 6903240 B2* (2005).

[13] Mertens M., Strohmaier K.G., Nurray P., Process for Manufacture of Molecular Sieves, *US. Pat. No. 7052664 B2* (2006).

[14] Gholamhosseiny M., Fatemi Sh., Rasoolzadeh M., Hydrogen Adsorption and Equilibrium Models on Multi-Walled Carbon Nanotubes at Moderate Temperatures and Pressures, *Inter. J. of Chem. Reac. Eng.*, **6**, p. 84 (2008).

[15] Tosheva, L., Valtchev, V.P., High-Silica Zeolite-β: From Stable Colloidal Suspensions to Thin Films, *Chem. Mat.*, **17**, p. 2494 (2005).

[16] Newalker B.L., Choudary N.V., Kumar P., Komarneni, S., Bhat, T.S.G., Exploring the Potential of Mesoporous Silica, SBA-15, as an Adsorbent for Light Hydrocarbon Separation, *Chem. Mater.*, **14**, p. 304 (2002).

[17] Li S., Falconer J.L., Noble R.D., SAPO-34 Membranes for CO2/CH4 Separation, *J. of Mem. Sci.*, **241**, p. 121 (2004).

[18] Li S., Falconer J.L., Noble R.D., SAPO-34 Membranes for CO2/CH4 Separation: Effect of Si/Al Ratio, *Micro. and Meso. Mat.*, **110**, p. 310 (2008).